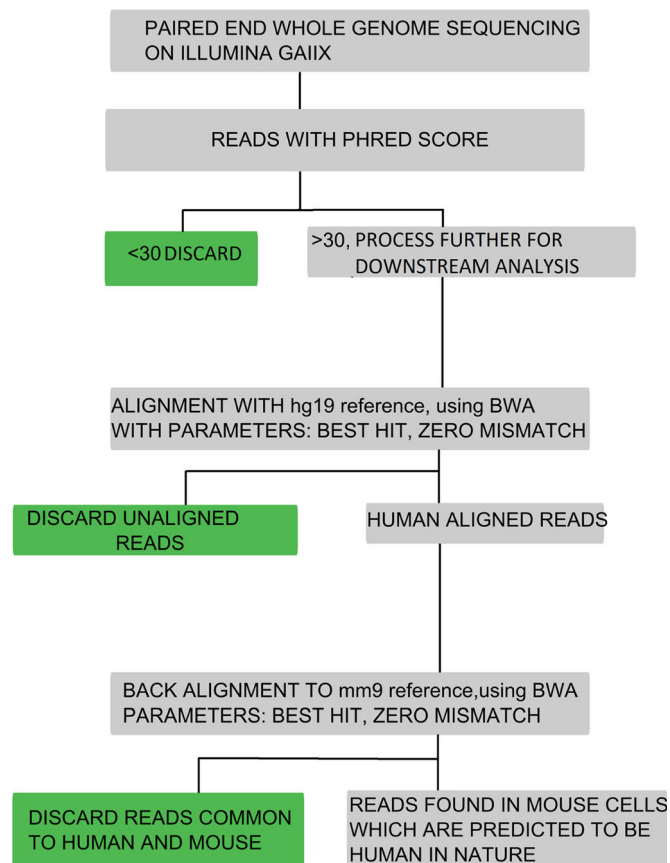


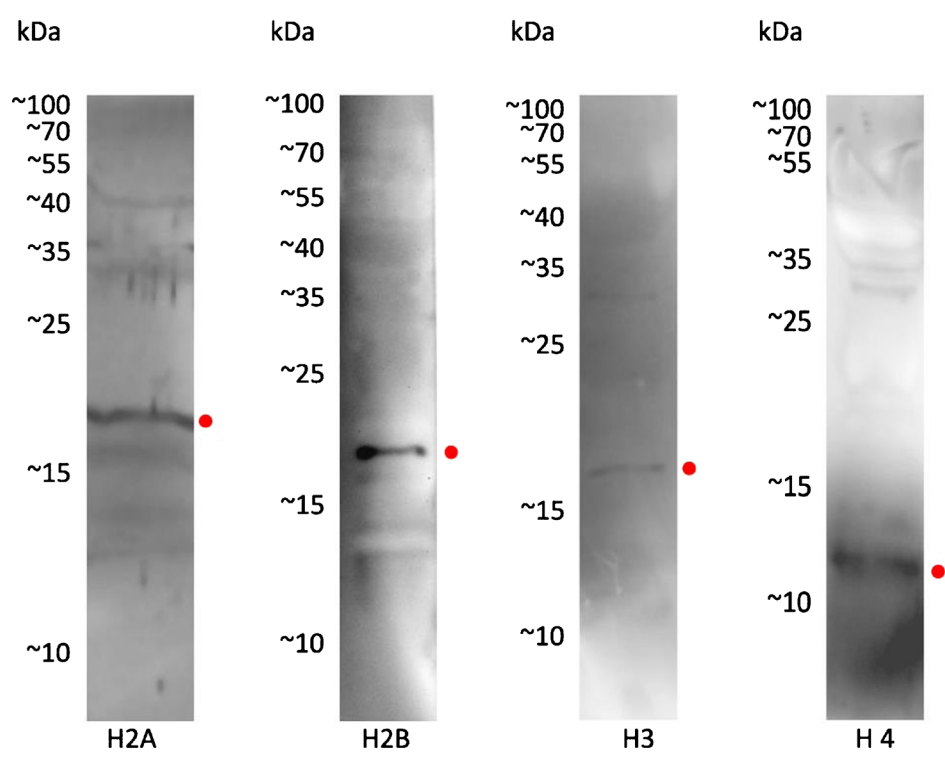
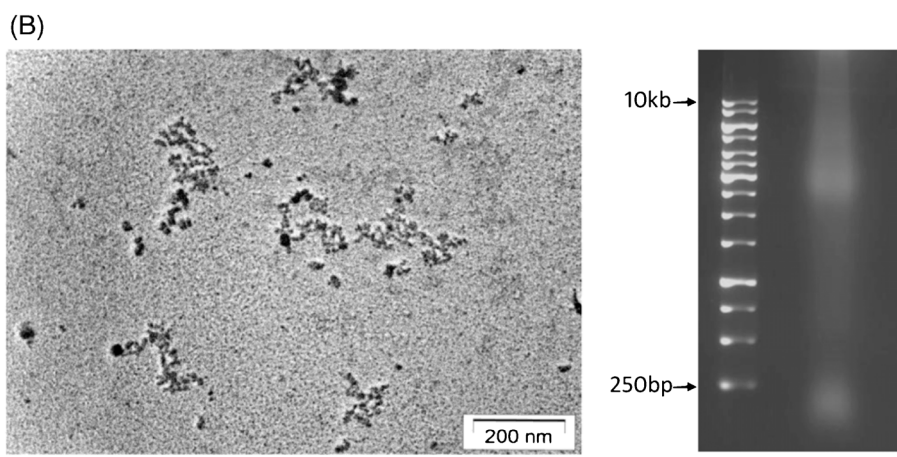
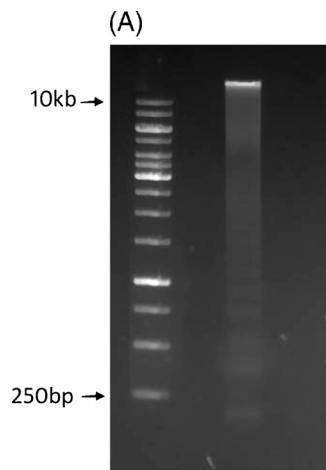
Circulating nucleic acids damage DNA of healthy cells by integrating into their genomes

INDRANEEL MITTRA, NAVEEN KUMAR KHARE, GORANTLA VENKATA RAGHURAM, ROHAN CHAUBAL, FATEMA KHAMBATTI, DEEPIKA GUPTA, ASHWINI GAIKWAD, PREETI PRASANNAN, AKSHITA SINGH, AISHWARYA IYER, ANKITA SINGH, PAWAN UPADHYAY, NAVEEN KUMAR NAIR, PRADYUMNA KUMAR MISHRA and AMIT DUTT

J. Biosci. 40(1), March 2015, 91–111, © Indian Academy of Sciences
Supplementary material

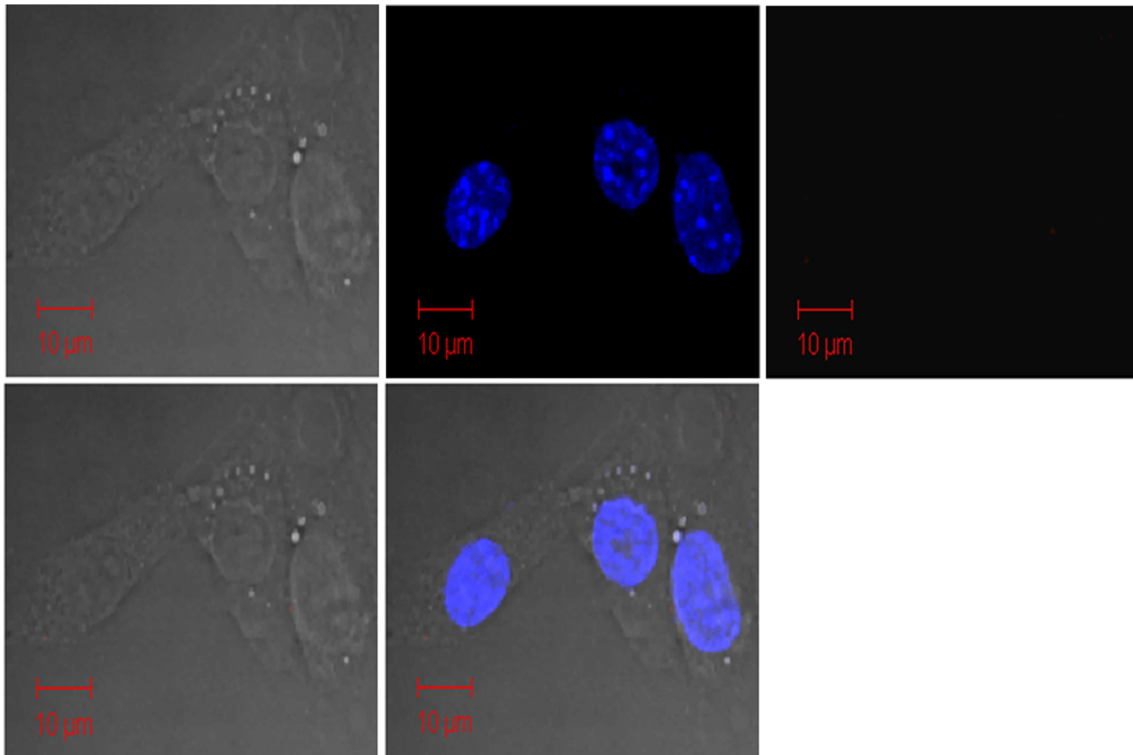


Supplementary figure 1. Subtractive computational algorithm to detect human genomic sequences from DNafs- and Cfs-derived mouse cell clones.

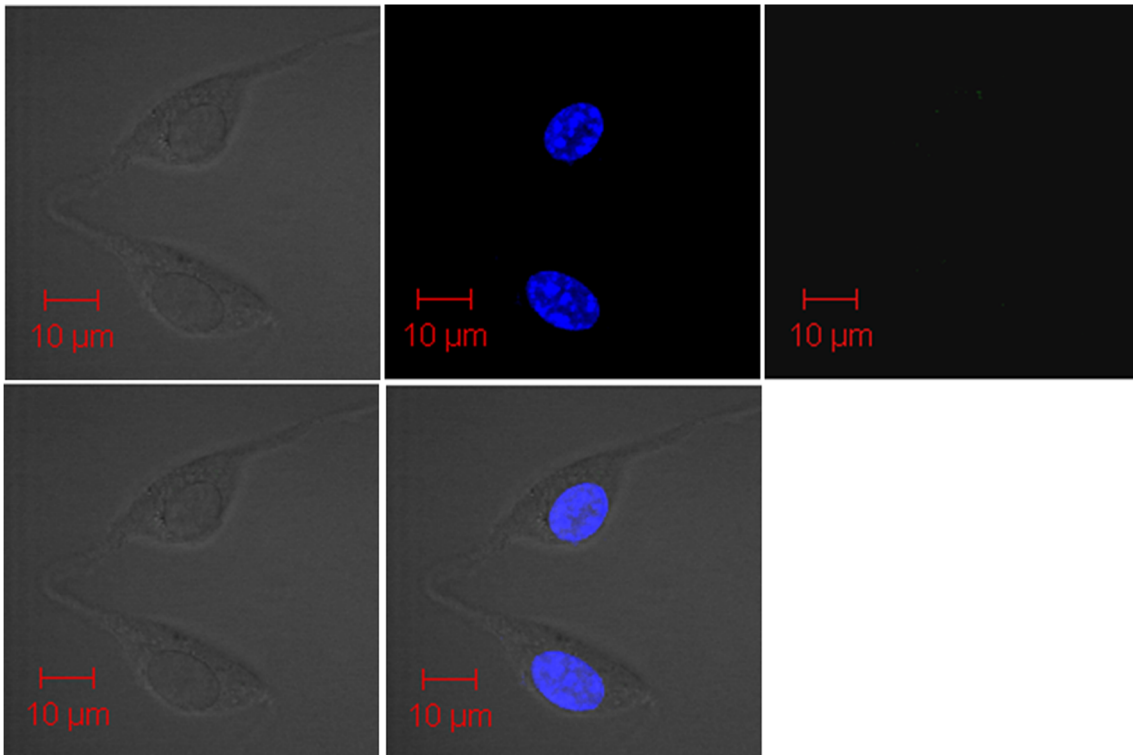


◀ **Supplementary figure 2.** Characteristic features of DNAs and Cfs isolated from plasma and serum respectively. **(A)** Agarose gel electrophoresis of DNAs (150 ng) isolated from plasma showing extensive size heterogeneity of DNA fragments with a suggestive ladder pattern. **(B)** Characteristic features of Cfs. Electron micrographs of Cfs showing typical beads-on-a-string appearance of chromatin of disparate sizes (upper left-hand panel). Agarose gel electrophoresis of DNA (150 ng) contained in Cfs showing extensive size heterogeneity of DNA fragments (upper right-hand panel). Western blot analysis using polyclonal antibodies against various histones showing presence of histone proteins in Cfs isolated from serum (lower panel). The H1 protein was not detectable in Cfs.

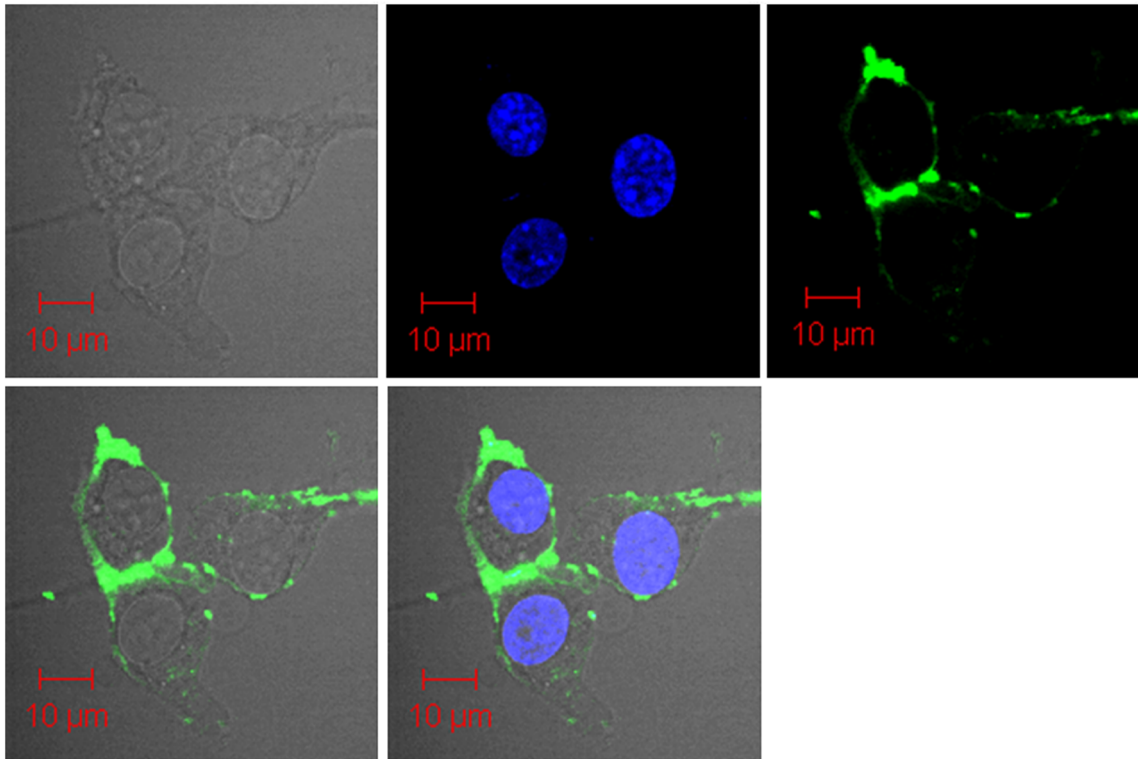
(A)



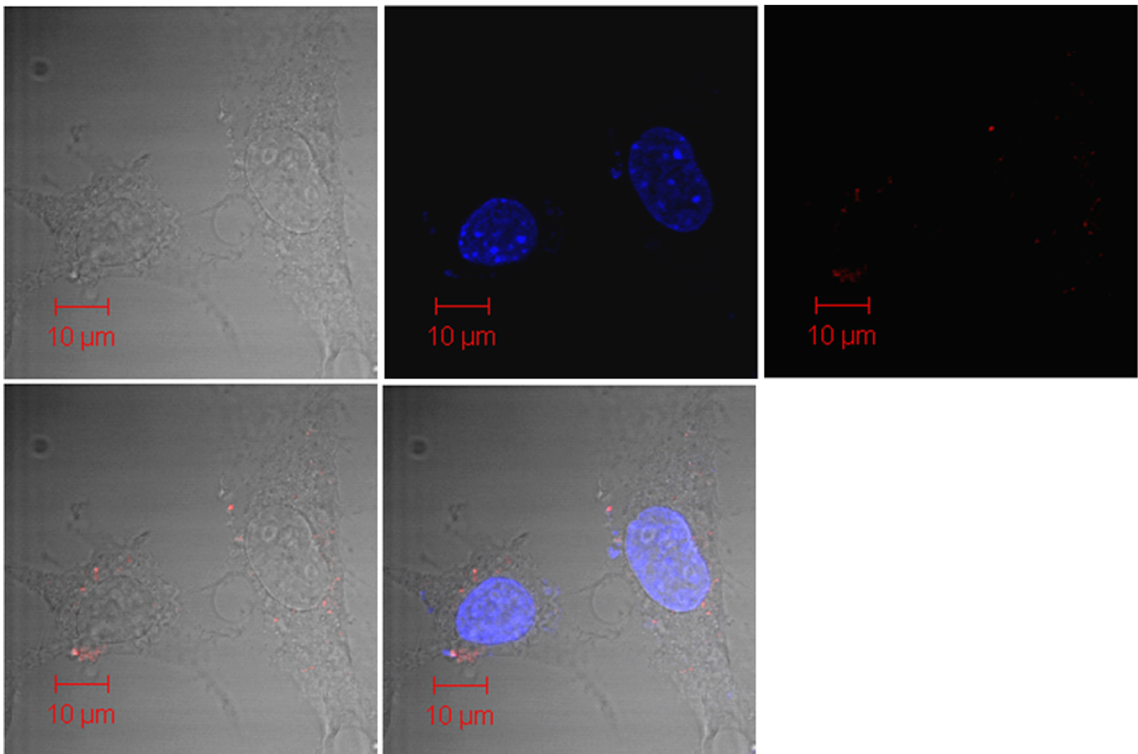
(B)



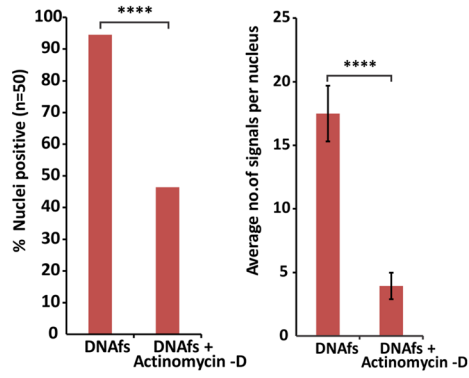
(C)



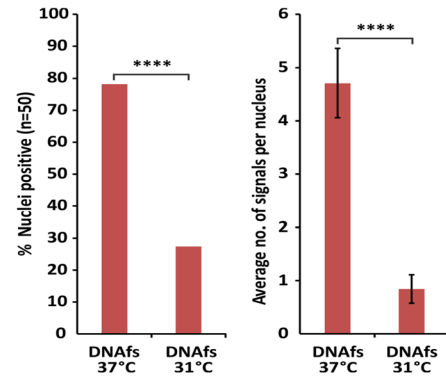
(D)



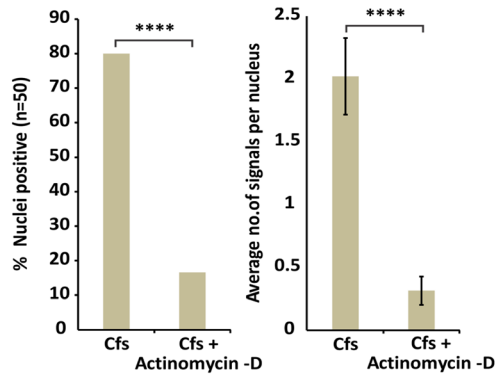
(E)



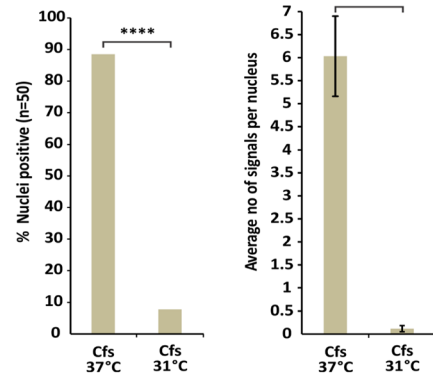
(G)



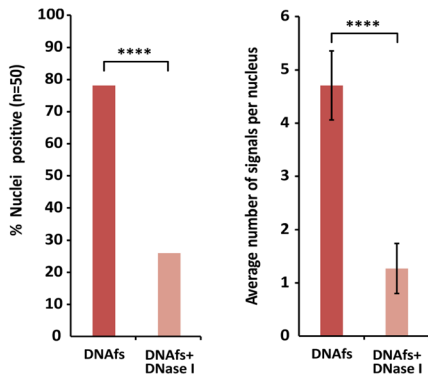
(F)



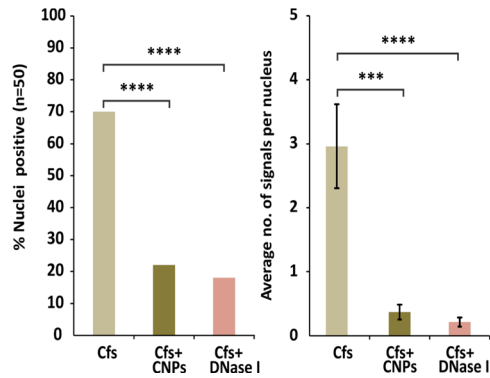
(H)



(I)

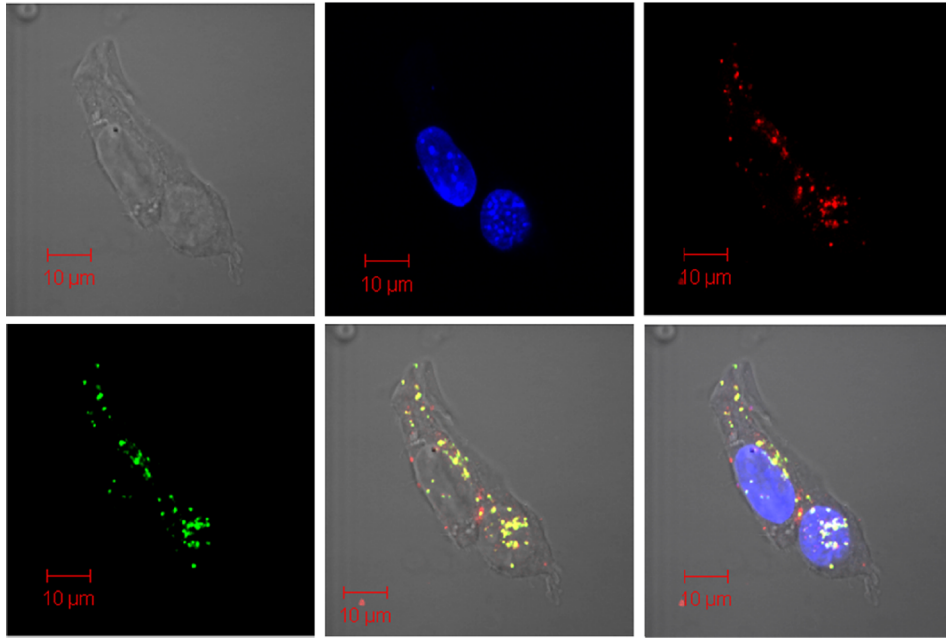


(J)

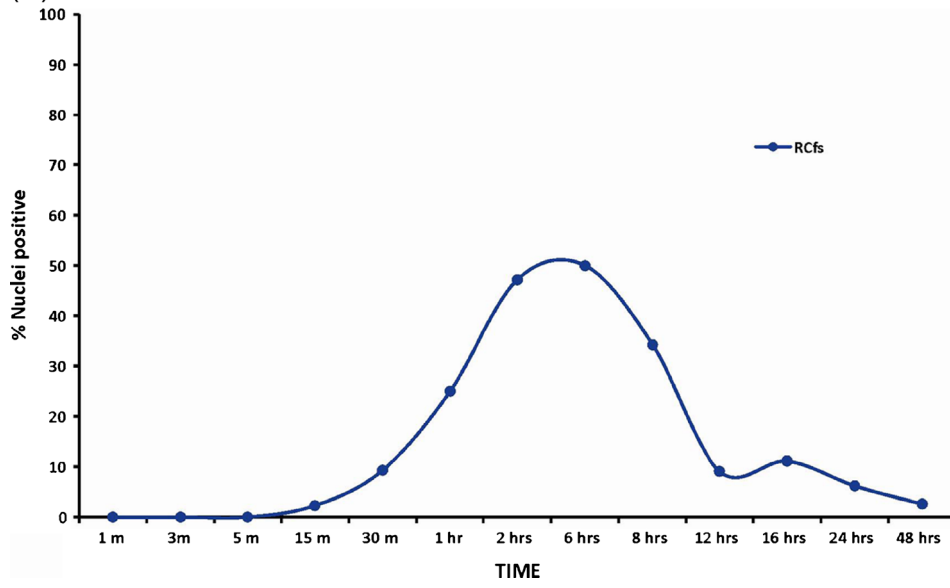


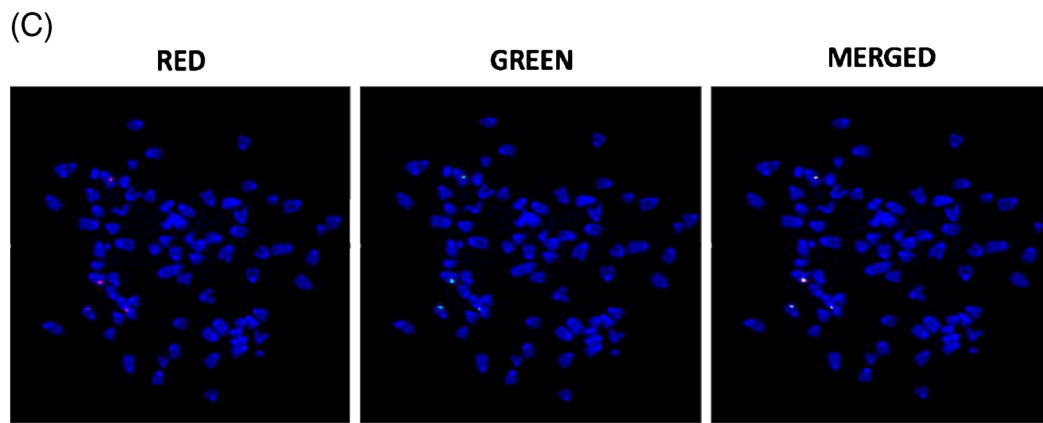
◀ **Supplementary figure 3.** Negative control experiments and those using specific inhibitors with respect to nuclear uptake and chromosomal association of DNAs and Cfs. (A) Nuclear uptake of labelled RNA. Semi-confluent NIH3T3 cells were treated for 6 h with Cy3-labelled RNA (10ng) purified from pooled plasma samples from cancer patients. Intracellular fate of labelled RNA was analysed by LSCM. A few low-intensity fluorescent signals are observed in the cytoplasm but not in the nuclei. (B) Nuclear uptake of labelled proteins. Cells plated as above were treated for 6 h with ATTO-TEC (green) labelled α -lactalbumin (10 ng). Intracellular fate of labelled protein was analysed by LSCM. None of the cells analysed (0/50) showed cytoplasmic or nuclear uptake of labelled protein. (C and D) Nuclear uptake of label alone. Cells plated as above were treated for 6 h with ATTO-TEC (green) and Platinum Bright (red) (1 μ L each) and analysed by LSCM. Both dyes, especially ATTO-TEC were seen in the cytoplasm but never in any of 50 nuclei examined. (E and F) Nuclear uptake of labelled DNAs and Cfs in presence of Actinomycin D. NIH3T3 cells (10×10^4) were treated with labeled DNAs and Cfs (5ng DNA each) for 6 h in the presence or absence of Actinomycin D (0.0005 μ g/mL); treated cells were examined under LSCM. Fifty nuclei were analysed in each case. Presence of Actinomycin D significantly reduced the number of nuclei showing positive fluorescent signals in case of both DNAs- and Cfs-treated cells (analysed by Chi-square test) as well as the average number of signals per nucleus (analysed by Student's *t*-test). (G and H) Nuclear uptake of labelled DNAs and Cfs at low temperature (31°C). Cells were plated as above and treated with labelled DNAs and Cfs (5ng DNA each) for 6 h at 31°C and 37°C; treated cells examined under LSCM. For experiments at low temperature, cells were kept at 31°C for 8 h prior to adding DNAs and Cfs. Fifty nuclei were analysed in each case. Cells grown at 31°C showed significantly reduced number of nuclei showing positive fluorescent DNAs and Cfs signals (analysed by Chi-square test) as well as the average number of signals per nucleus (analysed by Student's *t*-test) compared to those grown at 37°C. (I and J) Nuclear uptake of labelled DNAs and Cfs in presence of DNase I and/or CNPs. Cells were plated as above and treated with labelled DNAs and Cfs (5ng DNA each) for 6 h in the presence or absence of DNase I (0.05 U/mL) and/or CNPs (5 μ g H4 IgG /mL); treated cells examined under LSCM. Fifty nuclei were analysed in each case. In case of DNAs treated cells (supplementary figure 3I), DNase I treatment significantly inhibited the number of nuclei showing positive fluorescent DNAs signals (analysed by Chi-square test) as well as the average number of signals per nucleus (analysed by Student's *t*-test). With respect to Cfs (supplementary figure 3J), the number of nuclei showing positive fluorescent signals as well as the average number of signals per nucleus were inhibited by both DNase I and CNPs (analysed by Chi-square test and Student's *t*-test respectively. * $p < 0.05$, ** $p < 0.01$, *** $p < 0.001$, **** $p < 0.0001$).

(A)

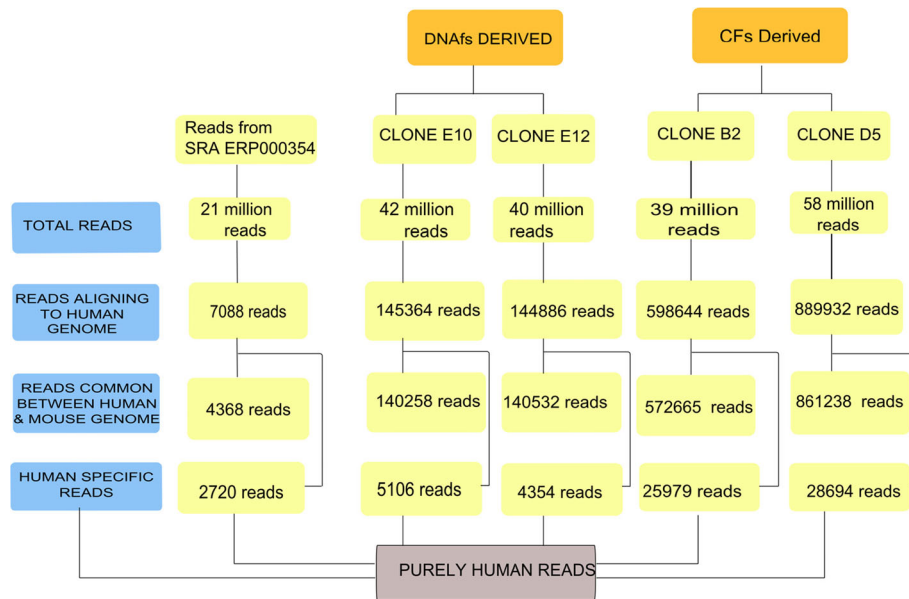


(B)





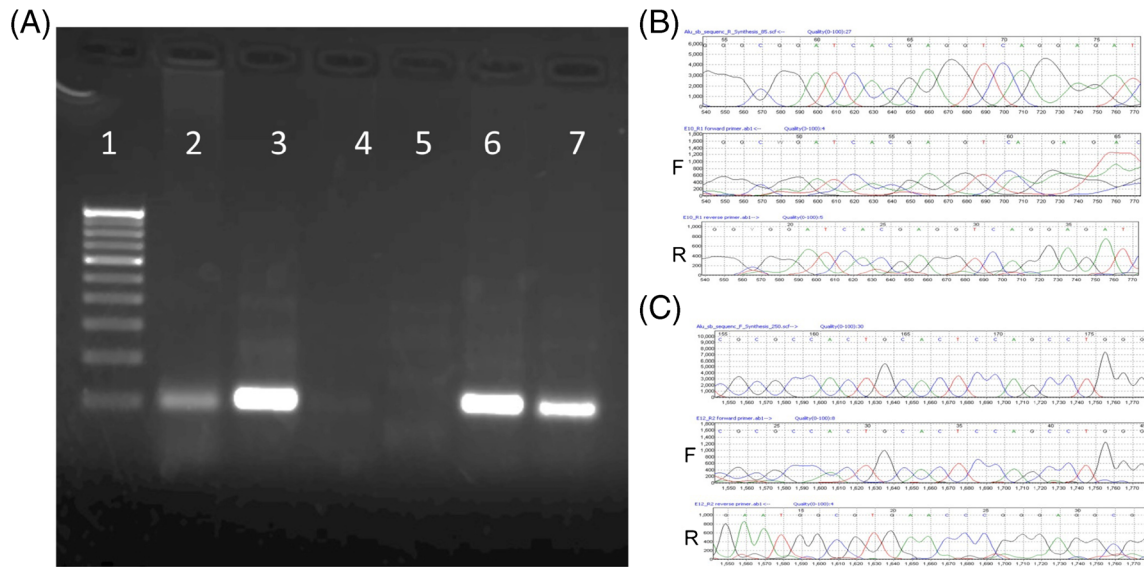
Supplementary figure 4. Cellular entry, kinetics of nuclear uptake and chromosomal association of fluorescently labelled RCfs. (A) NIH3T3 cells (10×10^4) were grown on cover-slips and treated with RCfs (10 ng DNA) dual-labelled with ULS (red) and ATTO-TEC (green) for 6 h and examined by LSCM. Presence of dual-labelled RCfs in the cytoplasm and nuclei are clearly seen. The red and green signals appear yellow in colour when the images are merged. (B) Kinetics of nuclear uptake of fluorescently labelled RCfs. NIH3T3 cells grown on cover-slips were treated with RCfs (10 ng DNA) and examined by LSCM at various time-points. Fifty nuclei were analysed at each time-point and those containing at least two fluorescent spots were counted as positive. (C) Association of fluorescently dual-labelled RCfs with chromosomes of treated cells. NIH3T3 cells were treated with RCfs (10 ng DNA) and metaphase spreads were prepared 6 h after treatment and analysed by fluorescence microscopy as described earlier.



Supplementary figure 5. Summary results of strictly human-specific sequences detected in single-cell clones generated from DNAs (E10, E12) and Cfs (B2, D5) treated NIH3T3 cells as well as in mouse reference genome through whole genome sequencing analysis. The 2720 sequence reads in reference genome are either an artifact of inefficiency of our alignment algorithm, or an artifact of sequencing in the mouse reference genome. The sequences represented by these 2720 reads were annotated and subsequently, all genes represented by these sequences were removed from our downstream analysis.

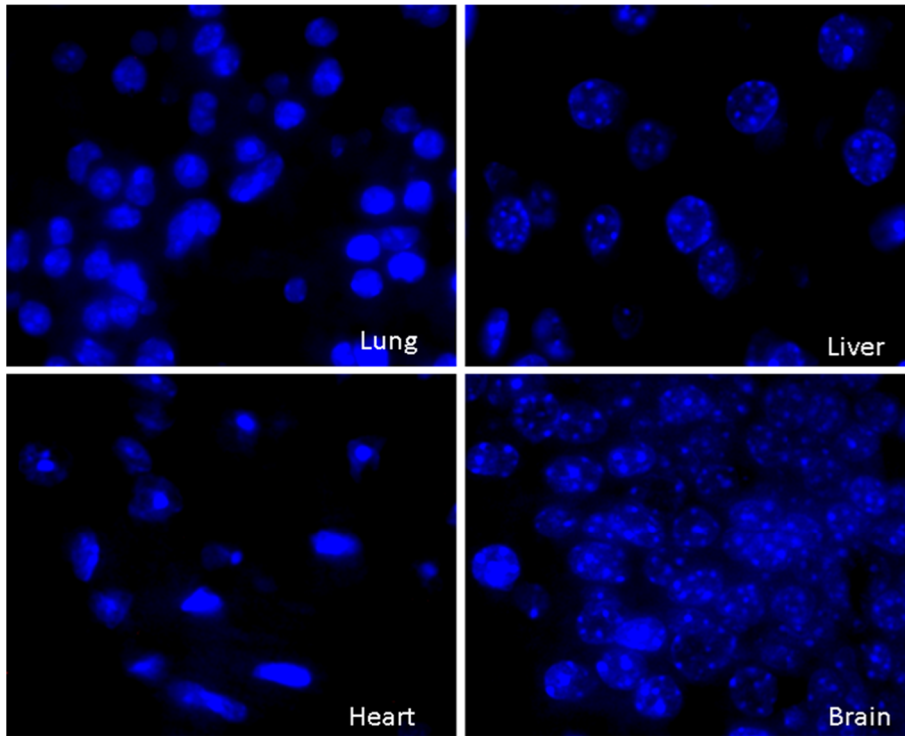
	Alu-J	Alu-Sx	Alu-Sq	Alu-Sc	Alu-Sp	Alu-FLA	Alu-Sb2	Alu-Sqpx	Alu-Sb
Cfs-derived clone B2	Red	Red	Red	Red	Red	Red	Red	Red	Red
Cfs-derived clone D5	Red	Red	Red	Red	Red	Red	Red	Red	Red
DNAs-derived clone E10	Red	Red	Red	Red	Red	White	White	White	White
DNAs-derived clone E12	Red	Red	Red	Red	Red	White	White	White	White
Total	39	28	27	13	9	3	3	1	1

Supplementary figure 6. Heat-map representation of *Alu* family members found in Cfs- and DNAs-derived clones: Distribution of all *Alu* elements with 80% and above sequence identity without gaps to the nucleotide sequences of all human *Alu* repeat elements database containing more than 1.1 million *Alu* repeats and 327 *Alu* family members is shown. Columns represent *Alu* family members found sorted in decreasing order from left to right by the last row that displays total number of *Alu* elements found for each family across all Cfs- and DNAs-derived clones – shown by rows. Red colour indicates presence of an *Alu* family member in the clone, white color indicates absence of *Alu* family member representation. Maximal occurrence of *Alu-Sx* and *Alu-J* family members (n=67 of 124 found across all clones) are known to be the most ancient and abundant *Alu* family constituting 850,000 repeats of 1.1 million in the human genome.

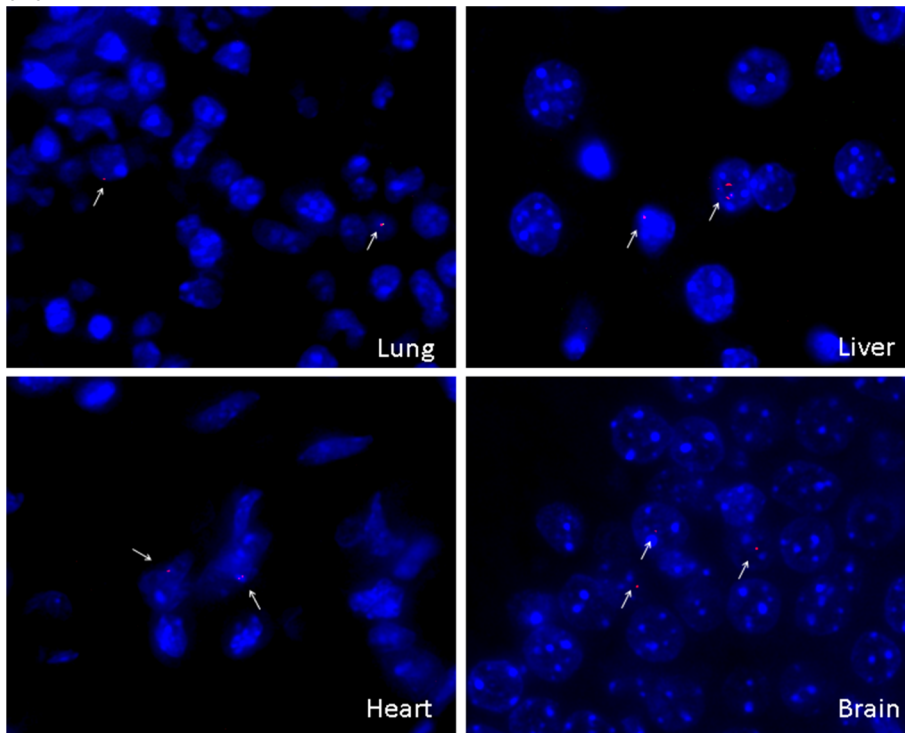


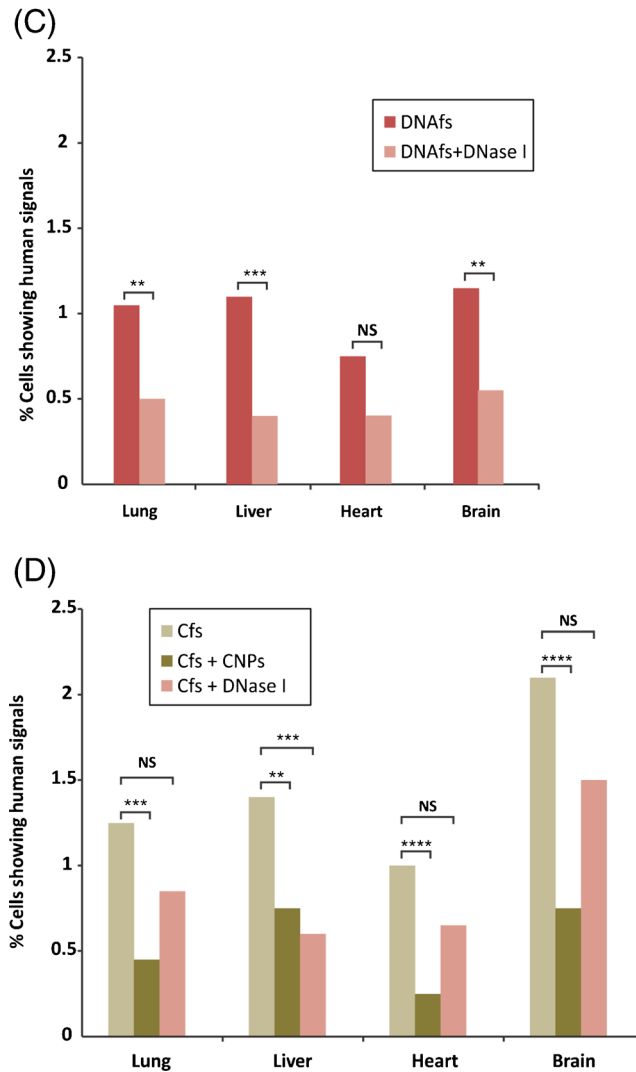
Supplementary figure 7. PCR detection and sequencing of human *Alu* elements in mouse clones derived from human Cfs and DNAs. Representative PCR amplification (A) and sequence trace (B and C) of *Alu-Sb* and *Alu-Sp*. (A) Lanes 2 and 3 correspond to PCR amplified *Alu-Sb* and *Alu-Sp* from D5 and E10 clones. Lanes 4 and 5 correspond to untreated NIH3T3 cells for amplification of *Alu-Sb* and *Alu-Sp*, respectively (negative control). Lanes 6 and 7 correspond to aliquots of a human cell DNA (positive control). (B and C) Sequence trace of amplified fragment *Alu-Sb* (B) and *Alu-Sp* (C) are displayed along with the reference human *Alu* sequence as generated by Mutation Surveyor.

(A)

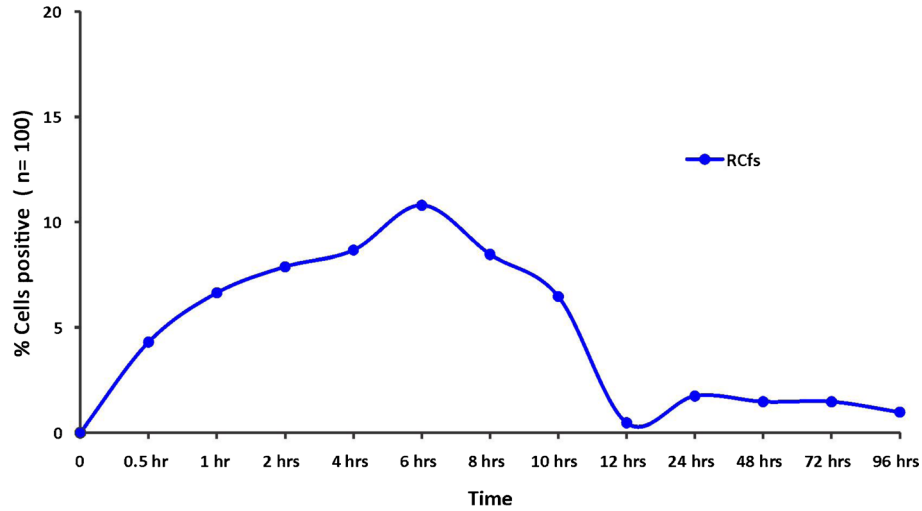


(B)

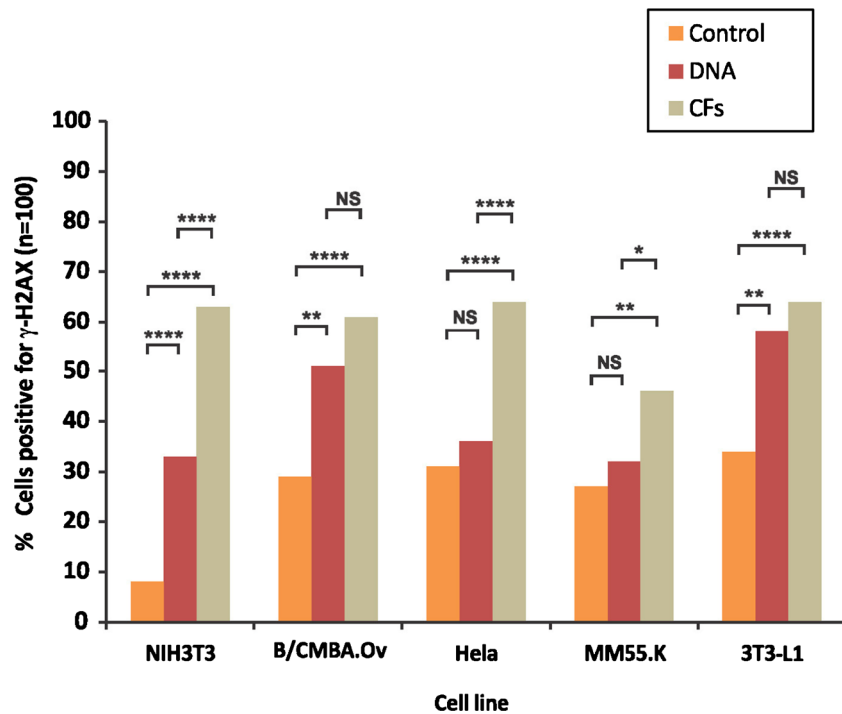




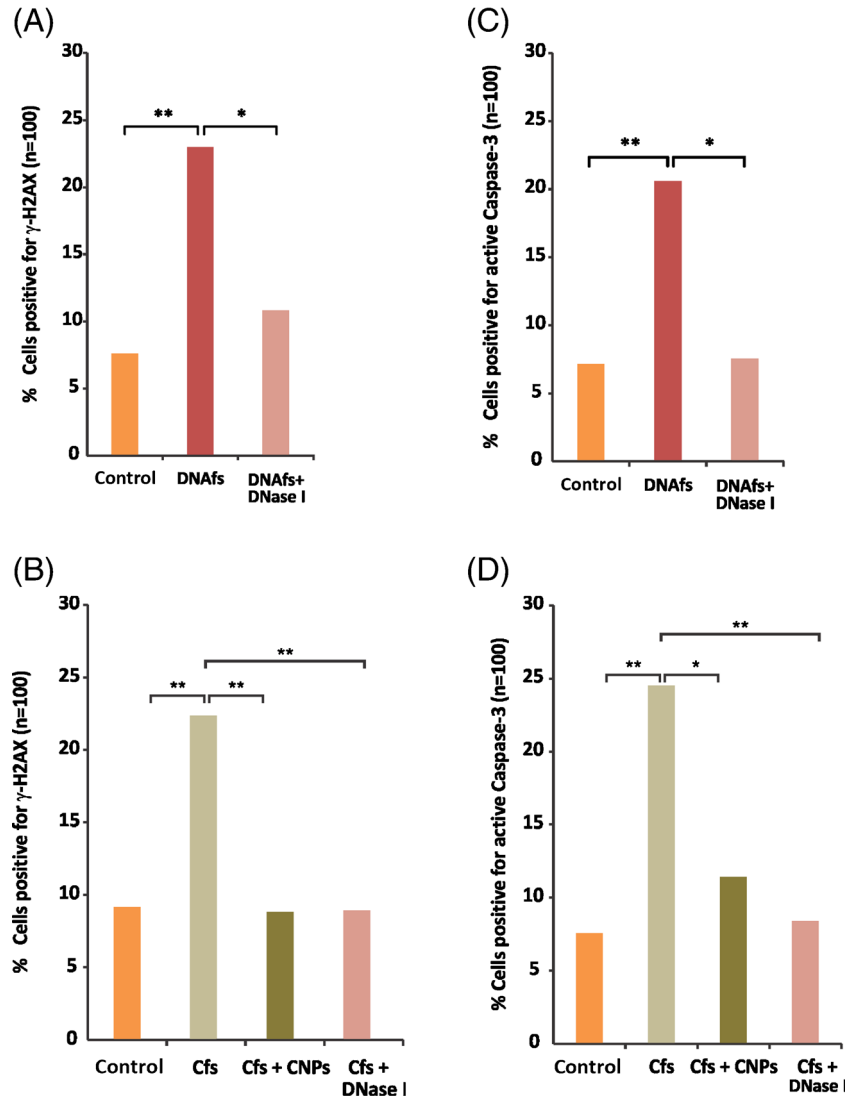
Supplementary figure 8. Detection of human DNA in cells of vital organs of mice by FISH following intravenous injections of DNafs and Cfs isolated from cancer patients. (A and B) Representative FISH images showing positive FISH signals in cells of vital organs of mice injected with Cfs (100 ng DNA) i.v. and sacrificed on day 7 (supplementary figure 8B). Untreated animals did not show any positive signals (supplementary figure 8A). (C and D) *In vivo* detection of human DNA by FISH in vital organs of mice following intravenous injection of DNafs and Cfs in presence or absence of DNase I and/or CNPs. Mice were given a single intravenous injection of DNafs and Cfs (100 ng DNA each) through tail vein with and without simultaneous administration of DNase I (15 mg/kg i.p.) and/or CNPs (50 μ g H4 IgG/mouse i.p.). DNase I and CNPs treatment was started 4 h prior to DNafs and Cfs administration and continued for 7 days. DNase I was injected at 12 hourly intervals while CNPs were administered every 24hr. Animals were sacrificed on day 7 and their vital organs, namely, heart, lung, liver and brain were removed and processed for FISH. The experiments were done in duplicate and with two animals in each group. Two thousand cells were counted for each tissue per animal and the percentage of nuclei showing human-specific signals (genomic and/or centromeric) was calculated and analysed by Chi-square test. Genomic integration of DNafs was inhibited by treatment with DNase I, while that of Cfs was inhibited by treatment with both DNase I and CNPs. * p <0.05, ** p <0.01, *** p <0.001, **** p <0.0001.



Supplementary figure 9. Kinetics of H₂AX phosphorylation in NIH₃T₃ cells treated with RCfs. NIH₃T₃ cells (10×10^4) grown on cover-slips were treated with RCfs (10ng DNA) and cells processed for immunofluorescence to detect H₂AX activation at various time points. Fifty nuclei in duplicate were analyzed at each time-point; those with two or more fluorescent foci were considered as positive.

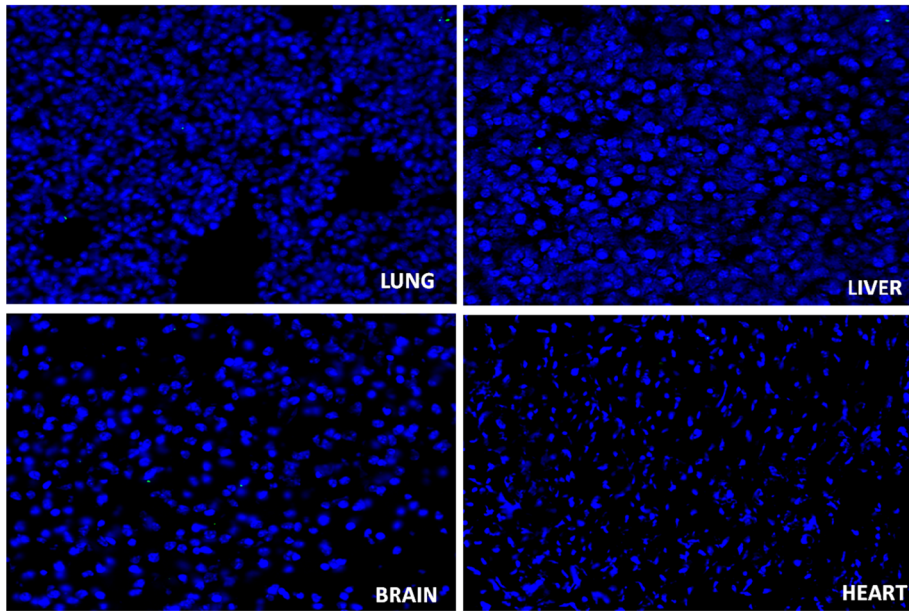


Supplementary figure 10. Induction of γ H₂AX in different cell lines in response to DNAs and Cfs. Cells (10×10^4) grown on cover-slips were treated with DNAs and Cfs (5 ng DNA each) and cells were processed for immunofluorescence at 6 hours following treatment. Experiments were done in duplicate, 50 cells were counted in each case and the percentage of cells showing positive signals was recorded. Number of nuclei with two or more fluorescent foci were counted as positive and analysed by Chi-square test. * $p < 0.05$, ** $p < 0.01$, *** $p < 0.001$, **** $p < 0.0001$. NIH3T3 = mouse fibroblast cells; B/CMBA.Ov = mouse ovary cells; HeLa = human cervical cancer; MM55.K = mouse kidney; 3T3-L1 = mouse adipocyte.

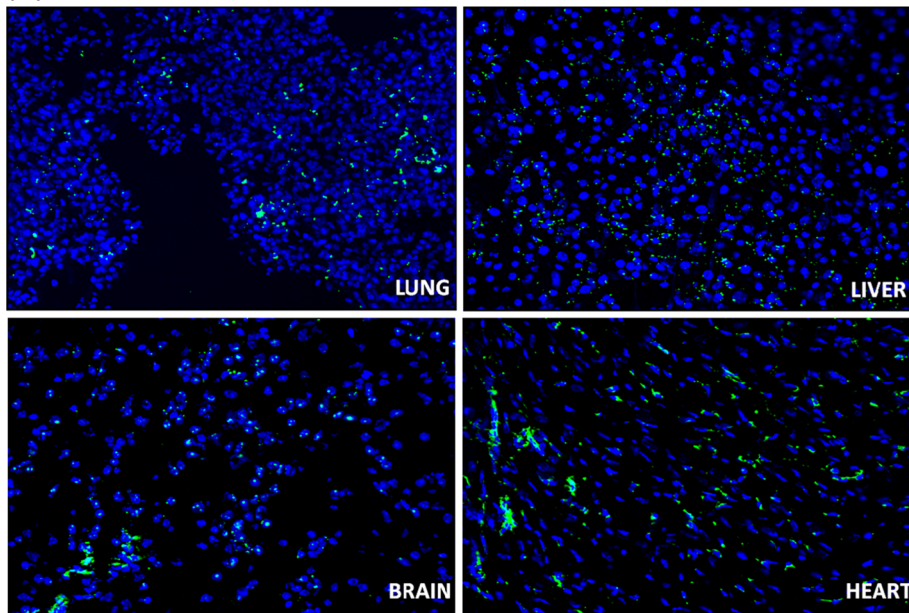


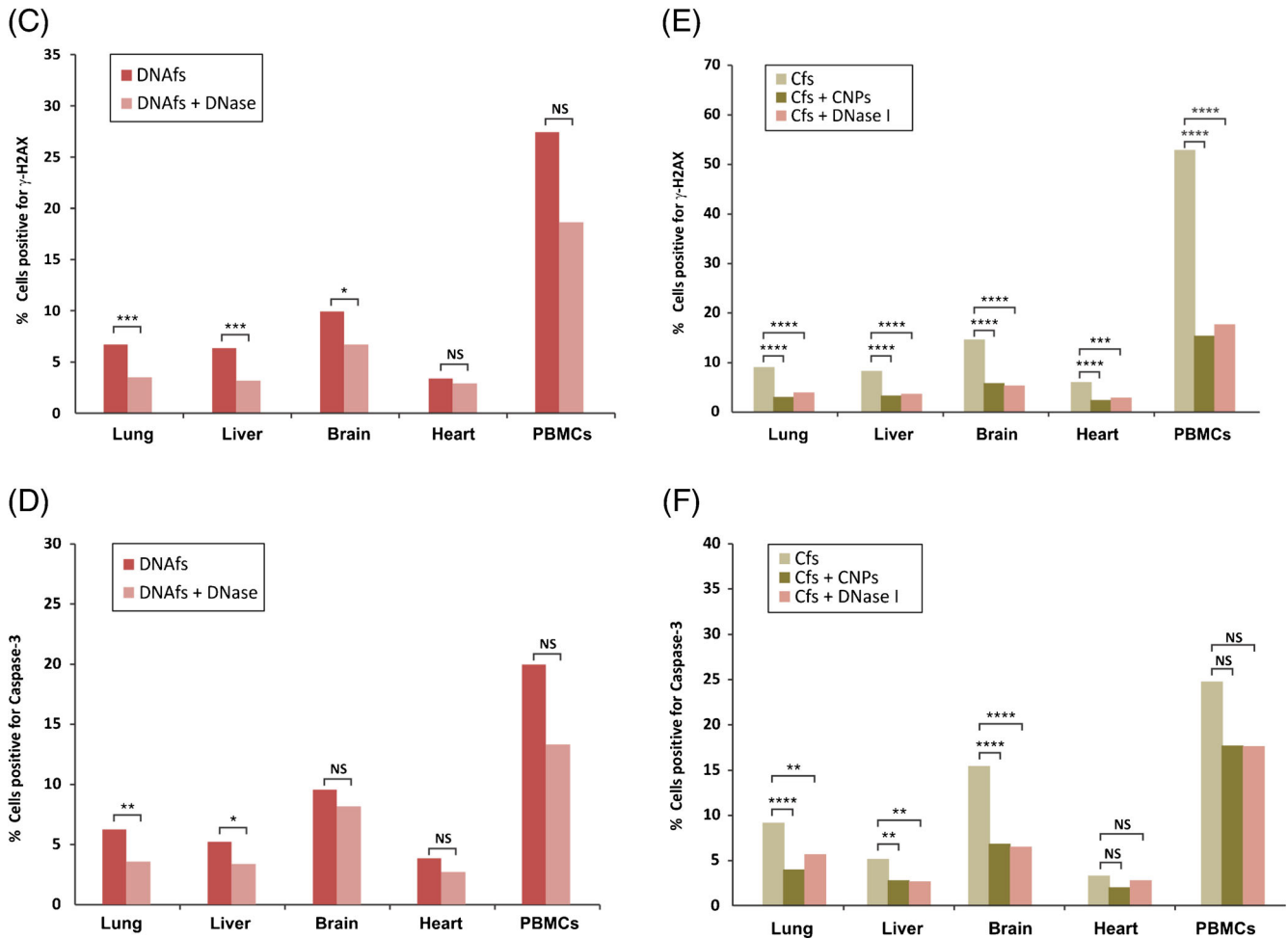
Supplementary figure 11. Inhibition of H2AX and Caspase-3 activation in response to DNafs and Cfs in NIH3T3 cells following treatment with DNase I and / or CNPs. NIH3T3 cells (10×10^4) grown on cover slips were treated with DNafs and Cfs (5 ng DNA each) in the presence or absence of DNase I (0.05 U/mL) and / or CNPs (5 μ g H4 IgG/mL). Cells were processed for immuno-fluorescence. Experiments were done in duplicate, 50 cells were counted in each case and the percentage of cells showing positive signals was recorded. Number of nuclei with two or more fluorescent foci were counted as positive and analysed by Chi-square test. (A–D) Both H2AX and Caspase-3 activation by DNafs was significantly inhibited by treatment with DNase I (A and C), while that by Cfs was significantly inhibited by treatment with both DNase I and CNPs (B and D). * $p < 0.05$, ** $p < 0.01$, *** $p < 0.001$, **** $p < 0.0001$.

(A)



(B)





Supplementary figure 12. Activation of H2AX and Caspase-3 in vital organs of mice following intravenous injections of DNAFs and Cfs isolated from cancer patients. (A and B) Representative immune-fluorescence images showing γ -H2AX activation in vital organs of mice following i.v. injection of Cfs. Cfs (100 ng DNA) were injected i.v. and animals were sacrificed after 24 h. Vital organs removed and processed for H2AX activation by immunofluorescence as described earlier. Animals treated with vehicle only (A); animals treated with Cfs (B). (C and D) Inhibition by DNase I of H2AX and Caspase-3 activation following intravenous injections into mice of DNAFs. Animals were injected with DNAFs (100 ng DNA) through tail vein with and without simultaneous administration of DNase I (15 mg/kg i.p.). DNase I treatment was started 4 h prior to DNAFs administration and repeated at 12 hourly intervals. Animals were sacrificed after 24hr and their vital organs, namely, heart, lung, liver and brain were removed and processed for immunofluorescence. The experiments were done in duplicate and with two animals in each group. At least 1000 DAPI-stained nuclei per animal were examined from 10 randomly chosen areas of various tissues, and in case of PBMCs, 100 nuclei per animal were examined. In both cases, the number of nuclei showing positive foci (γ -H2AX) and number of nuclei showing positive fluorescence (Caspase-3) were recorded and analysed by Chi-square test. Both H2AX and Caspase-3 activation following DNAFs treatment were inhibited by concurrent treatment with DNase I. (E and F) Inhibition by DNase I and/or CNPs of H2AX and Caspase-3 activation following intravenous injections into mice of Cfs. Mice were given a single intravenous injection of Cfs (100 ng DNA) through tail vein with and without simultaneous administration of DNase I (15 mg/kg i.p.) and/or CNPs (50 μ g H4 IgG/mouse i.p.). DNase I and CNPs treatment was started 4 h prior to Cfs administration; DNase I was injected at 12 hourly intervals thereafter while CNPs were administered once 24 h after the first injection. Animals were sacrificed after 24 h and their vital organs, namely, heart, lung, liver and brain were removed and processed for immunofluorescence. The experiments were done in duplicate and with two animals in each group. At least 1000 DAPI-stained nuclei per animal were examined from 10 randomly chosen areas of various tissues, and in case of PBMCs, 100 nuclei per animal were examined. In both cases, the number of nuclei showing positive foci (γ -H2AX) and number of nuclei showing positive fluorescence (Caspase-3) were recorded and analysed by Chi-square test. H2AX and Caspase-3 activation following Cfs treatment were inhibited by treatment with both DNase I and CNPs. * p <0.05, ** p <0.01, *** p <0.001, **** p <0.0001.

Supplementary table 1. Details of cancer patients

Sr. No.	Age	Sex	Type of cancer	Stage
1	68	M	Ca-Oesophagus	III
2	36	F	Ca-Breast	III
3	40	F	Ca-Breast	III
4	47	F	Ca-Breast	III
5	46	F	Ca-Breast	III
6	45	F	Ca-Breast	IV
7	48	F	Ca-Breast	III
8	48	F	Ca-Breast	III
9	53	F	Ca-Breast	III
10	33	M	Acute myeloid leukemia-M2	Poor risk
11	54	M	Ca-Supraglottis	III
12	58	F	Ca-Breast	III
13	50	F	Ca-Breast	III
14	60	M	Ca-Esophagus	III
15	54	M	Acute myeloid leukemia-M2	Poor risk
16	53	M	Ca-Hypopharynx	III
17	44	M	Carcinoid Tumour	III
18	53	F	Acute myeloid leukemia-M4	Good risk
19	47	M	Ca-Lung	IV
20	47	F	Ca-Breast	III
21	25	M	Acute myeloid leukemia-M0	Poor risk
22	46	F	Ca-Breast	III
23	45	F	Ca-Breast	III
24	50	F	Ca-Breast	III
25	47	F	Ca-Breast	III
26	53	F	Ca-Breast	III
27	49	F	Ca-Breast	III
28	56	F	Ca-Oesophagus	III
29	48	F	Ca-Breast	III
30	44	F	Ca-Breast	III
31	54	M	Ca-Lung	III
32	49	F	Ca-Breast	III
33	36	F	Ca-Breast	III
34	56	F	Ca-Breast	III
35	48	F	Ca-Breast	III
36	72	F	Ca-Breast	III
37	46	F	Ca-Breast	III
38	37	F	Ca-Breast	III
39	43	F	Ca-Breast	III
40	56	F	Ca-Breast	III
41	59	F	Ca-Breast	III
42	72	F	Ca-Oesophagus	III
43	53	M	Ca-Buccal Mucosa	IV
44	49	F	Ca-Breast	III
45	51	F	Ca-Ovary	III
46	17	F	Acute myeloid leukemia-M4	Good risk

Sr. No.	Age	Sex	Type of cancer	Stage
47	38	F	Acute myeloid leukemia-M2	Good risk
48	48	F	Ca-Breast	III
49	30	F	Ca-Breast	III
50	59	M	Ca-Oesophagus	III
51	47	F	Ca-Ovary	III
52	34	M	Ca-Stomach	IV
53	54	F	Ca-Ovary	III
54	41	F	Ca-Stomach	IV
55	50	F	Ca-Ovary	III
56	40	M	Ca-Buccal Mucosa	IV
57	62	F	Ca-Oesophagus	III
58	56	M	Ca-Gingivo-Buccal Sulcus	III
59	62	M	Ca- Gingivo-Buccal Sulcus	III
60	55	M	Hodgkin's Lymphoma	IV
61	46	F	Ca-Breast	III
62	32	F	Ca-Breast	III
63	57	F	Ca-Breast	III
64	50	F	Ca-Breast	III
65	50	F	Ca-Breast	III
66	42	F	Ca-Breast	III

Mean age = 48.15 ± 9.70 (mean \pm SD)

Details of healthy volunteers

Sr. No.	Age	Sex
1	52	F
2	50	F
3	50	F
4	51	F
5	52	F
6	42	F

Mean age = 49.50 ± 3.78 (mean \pm SD)

Supplementary table 2. Summary of sequencing reads generated from Cfs-derived and DNAFs-derived clones using second-generation sequencing platform (we achieved a mean sequencing coverage of 1.2x across the four clones)

Clone	Sequence File	Read length	No of Sequences	No of Bases	Coverage
E10 DNAFs-derived	E10 Forward	100	21,379,060	2,137,906,000	1.57
	E10 Reverse	100	21,379,060	2,137,906,000	
	Total		42,758,120	4,275,812,000	
E12 DNAFs-derived	E12 Forward	100	20,153,181	2,015,318,100	1.48
	E12 Reverse	100	20,153,181	2,015,318,100	
	Total		40,306,362	4,030,636,200	
B2 Cfs-derived	B2 Forward	54	19,571,148	1,056,841,992	0.77
	B2 Reverse	54	19,571,148	1,056,841,992	
	Total		39,142,296	2,113,683,984	
D5 Cfs-derived	D5 Forward	54	29,094,305	1,571,092,470	1.15
	D5 Reverse	54	29,094,305	1,571,092,470	
	Total		58,188,610	3,142,184,940	

Supplementary Table 3. List of DDR and apoptotic pathway antibodies and their sources

Antibody	Source	Catalogue No.
(p-Ser139) γ -H2AX	Abcam®, UK	Ab26350
(p-Ser 428)-ATR	Abcam®, UK	Ab2905
(p-Ser1981) ATM	Abcam®, UK	Ab2888
MDC-1	Abcam®, UK	Ab11169
(p-Ser 20) p-p53	Santa Cruz Biotechnology Inc., USA	SC18078-R
(pThr145) p-p21	Santa Cruz Biotechnology Inc., USA	SC-20220-R
GADD34	Abcam®, UK	Ab9869
Nibrin	Santa Cruz Biotechnology Inc., USA	SC11431
Rad50	Santa Cruz Biotechnology Inc., USA	SC7675
Mre11	Cell Signalling Technology®, USA	#4895
(p-Ser 2056) DNA-PKcs	Abcam®, UK	Ab32566
DNA ligase IV	Abcam®, UK	Ab80514
Cytochrome-C	Millipore, USA	05-479
active Caspase-3	Abcam®, UK	Ab4051

Supplementary table 4. Tabulation of human *Alu* elements detected in Cfs and DNAFs-derived NIH3T3 clones

Clones	Total <i>Alu</i> sequences	Unique <i>Alu</i> families
Cfs-derived B2	47	8
Cfs-derived D5	35	8
DNAFs-derived E10	19	5
DNAFs-derived E12	23	5

Unique *Alu* families represent the families of the *Alu* sequences detected in the clones. The total *Alu*sequences found in the Cfs and DNAFs derived clones were depleted by the reads found in the control.